Smoluchowski thermostat: A realistic introduction of the tangential momentum accommodation coefficient

Martijn G. Verbeek*
Dibbitsstraat 12, 1689 EE, Zwaag, The Netherlands
(Received 31 December 2008; revised manuscript received 16 February 2010; published 12 April 2010)

This work presents a simulation technique that can be used to compute the thermal interaction between a gas and a cylindrically shaped wall. The method is computationally simple and is based on the Maxwell-Smoluchowski thermal wall scenario often used for the slit pore geometry. A geometric argument is used to find the corresponding thermalization mechanism for the cylindrical confinement. The algorithm serves as a thermostat, which enables one to perform constant-temperature simulations. By means of simple numerical simulations, Smoluchowski's expression for self-diffusivity D_s is then recovered in reduced units. The tangential momentum accommodation coefficient is interpreted as a coupling constant for the thermostat similar to the one used for the ordinary Andersen thermostat but applied locally onto the boundary crossing particles.

DOI: 10.1103/PhysRevE.81.046701 PACS number(s): 02.70.Ns, 34.35.+a

I. INTRODUCTION

Diffusion of gases within simple nanopores is an area of research of practical importance due to the rising interest in diffusion in carbon nanotubes [1–3]. If the mean-free path of the gas particles exceeds the pore diameter, kinetic theory based on the Chapman-Enskog normal solution [4] is expected to break down and the coefficient of self- (or tracer) diffusion D_s becomes density independent. In the (extreme) low-density regime gas-gas interactions can be neglected and diffusion is fully quantified by tracer diffusion. A century ago Knudsen derived a simple equation for the density independent tracer diffusion of a rarefied gas confined within a cylindrical pore [5]. Knudsen assumed all gas-wall collisions were governed by the cosine law of reflection [6]. Smoluchowski later generalized the model by including Maxwell's assumption that only a fraction f of the total number of collisions was scattered diffusely, while the remainder $1-f$ is reflected specularly [7,8]. This fraction is the tangential momentum accommodation coefficient (TMAC). The TMAC governs the degree of slip at the surface. The physical picture of the Smoluchowski model has gained interest due to applications in gas separations. For instance, Arya was able to show that gases having the same nominal properties (mass, viscosity, density) but different accommodation coefficients may be kinetically separated in the Knudsen regime [9]. In order to achieve efficient separation a detailed understanding of the mechanism describing the gas-wall collision is necessary. Two types of simulations are often used to solve this problem. The first type involves molecular dynamics (MD) simulations in which the wall consists of atoms that interact with the gas via a Lennard-Jones type of potential. Arya was able to relate the coefficient f to the parameters of the Lennard-Jones potential by looking at the reflected and the incoming drift velocity [9]. Jakobtorweihen *et al.* calculated f via the ratio between the number of diffusive collisions and the total number of collisions at the gas-wall surface [2].

In the second type of simulations the gas-wall interaction is modeled by a simple reflection law. As mentioned by Celestini *et al.* there is no suitable way of introducing f in these so-called "billiardlike simulations" (BLS) [10]. An interesting example of BLS is the thermal wall scenario, used by Tenenbaum *et al.* to study the limit of validity of Fourier's law [12]. The thermal wall scenario states that whenever a gas particle crosses a boundary it is emitted back from the wall with a velocity drawn from a particular distribution at a given wall temperature. Thermal walls have been successfully implemented for the slit pore geometry where they have been mainly used to generate stationary nonequilibrium states [12,13].

II. THEORETICAL BACKGROUND

The goal of this research is to show that the TMAC can be introduced in a more natural manner for BLS, by constructing a thermal wall for the cylindrical geometry. The procedure starts by considering a cylinder where periodic boundary conditions are applied in the z-direction. The cylinder has diameter d and length L. The nonperiodic xy-plane is now considered. If the thermostat is switched off and a particle would cross the boundary, a specular reflection would produce a velocity, $\vec{v}^{spec}=(v_x^{spec},v_y^{spec})$

$$\vec{v}^{spec}=\vec{v}^{in}-2(\vec{v}^{in}\cdot\hat{n})\hat{n}, \tag{1}$$

where $\hat{n}=\frac{1}{r}(x,y)$ and $\vec{v}^{in}=(v_x^{in},v_y^{in})$ is the incoming velocity. A specular collision would leave the z-component of the velocity unaltered. A position update in the xy plane would bring the particle back to side of the wall from which it came. If the thermostat is switched on one considers an additional step. Suppose a gas particle located at the wall has position $\vec{r}=(x,y)$ in the nonperiodic xy plane, with $|\vec{r}|=\frac{d}{2}-O(\Delta t)$. The particle has been brought back via a specular collision, after which a thermostat has scattered the particle diffusively. The particle now has an arbitrary velocity $\vec{v}^{ran}=(v_\perp,v_\parallel,v_z)$. The parallel components of this velocity, $(v_\parallel,v_z)$, do not change upon a specular collision. They have been drawn out of a Maxwell velocity distribution

*gustafverbeek@gmail.com

$$f(v_{\parallel}) = \sqrt{\frac{m}{2\pi k_B T_w}} \exp\left[\frac{-mv_{\parallel}^2}{2k_B T_w}\right]. \tag{2}$$

The orthogonal/normal component flips sign upon a specular collision and was sampled out of the following distribution [11–13]

$$f(v_{\perp}) = \frac{m}{k_B T_w} v_{\perp} \exp\left[\frac{-mv_{\perp}^2}{2k_B T_w}\right], \tag{3}$$

where T_w is the wall/thermostat temperature. The thermalization mechanism described by the Eqs. (2) and (3) was proposed by Tenenbaum to study heat transfer in the slit pore geometry [12,13]. Recently, Celestini *et al.* noticed that Eq. (3) is compatible with the cosine law of diffuse scattering [10], but perhaps it is easier to introduce this equation via the gas-wall collision frequency. Equation (3) is used if one wants to sample the flux of particles hitting the wall [14,15]. This flux is determined by the number of particles present in the volume $v_{\perp} dt dS$; i.e.,

$$dN^{hit}(t+dt, v_{\perp}+dv_{\perp}) = \rho \sqrt{\frac{m}{2\pi k_B T}} \times \exp\left(-\frac{mv_{\perp}^2}{2k_B T}\right) v_{\perp} dv_{\perp} dt dS, \tag{4}$$

with $v_{\perp} \epsilon [0,\infty)$. One can multiply with and divide by $4k_B T/m$ in order to obtain the following expression for the particle flux

$$dN^{hit}(t+dt, v_{\perp}+dv_{\perp}) = \frac{\rho}{4} v^{thermal} \frac{m}{k_B T} v_{\perp} \times \exp\left(-\frac{mv_{\perp}^2}{2k_B T}\right) dv_{\perp} dt dS, \tag{5}$$

where $v^{thermal} = \sqrt{8k_B T/\pi m}$. By defining $f(v_{\perp})$ via Eq. (3), the following shorthand notation is possible:

$$dN^{hit}(t+dt, v_{\perp}+dv_{\perp}) = \frac{\rho}{4} v^{thermal} f(v_{\perp}) dv_{\perp} dt dS \tag{6}$$

The normal component of the velocity can now be integrated over the range $[0,\infty)$. This integral is the normalization condition or zeroth moment of $f(v_{\perp})$ and equals one. It is also possible to integrate over the surface dS. If it is assumed that the local density to some approximation can be written as a constant,

$$\rho = \frac{N}{V} = \frac{4N}{\pi d^2 L}, \tag{7}$$

then the surface integration delivers a factor πdL, which is the surface area of the cylinder. Substitution of the approximation for the local density and carrying out the integration at the same time produces

$$dN^{hit}(t, t+dt) = \frac{N}{d} v^{thermal} dt. \tag{8}$$

The gas-wall collision frequency is then

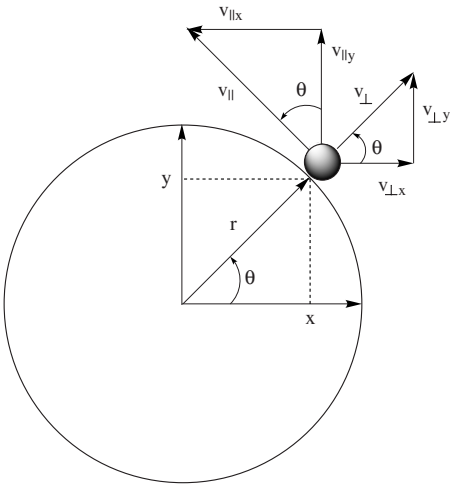

FIG. 1. Decomposition of $\vec{v}_{\perp}$ and $\vec{v}_{\parallel}$ into the x and y component.

$$\nu^{gw} = \frac{N}{d} v^{thermal}, \tag{9}$$

where N is the number of particles present and d is the cylinder diameter. This result will be tested with numerical simulations.

The angle of reflection is obtained by transforming the set $(v_{\parallel}, v_{\perp})$ into (v_x, v_y) (the z component is not transformed). This is realized by treating the components $v_{\parallel}$ and $v_{\perp}$ as vectors with a x and y component. In Fig. 1 a sketch is given of the decomposition. A quick inspection of Fig. 1 shows that

$$v_{\perp,x} = v_{\perp} \cos\theta = v_{\perp} \frac{x}{r}$$

$$v_{\perp,y} = v_{\perp} \sin\theta = v_{\perp} \frac{y}{r}, \tag{10}$$

where $r = \sqrt{x^2+y^2}$. A similar analysis can be applied onto $\vec{v}_{\parallel}$ yielding $(v_{\parallel,x}, v_{\parallel,y})$. The total x-component of the velocity, v_x^{ref}, is the sum of $v_{\parallel,x}$ and $v_{\perp,x}$; i.e.,

$$v_x^{ref} = v_{\perp} \frac{x}{r} - v_{\parallel} \frac{y}{r}. \tag{11}$$

This procedure can be repeated to give an expression for v_y^{ref}. In Fig. 1 the arbitrary velocity in the xy-plane is drawn with the same sign as the outward normal unit vector $\hat{n}$. The reflected velocity must have the opposite sign. This is achieved by flipping the sign of the $v_{\perp}$ component of v_x^{ref} and v_y^{ref}. Thus, in order to guarantee $\vec{v}^{ref} \cdot \hat{n} < 0$, one is left with

$$v_x^{ref} = -v_{\perp} \frac{x}{r} - v_{\parallel} \frac{y}{r}. \tag{12}$$

There is no need to flip the sign of v_z^{ref} and this component is directly sampled from Eq. (2). The reflected velocities upon a diffusive gas-wall collision are given by

$$\begin{pmatrix} v_x^{ref} \\ v_y^{ref} \\ v_z^{ref} \end{pmatrix} = \frac{1}{r}\begin{pmatrix} -x & -y & 0 \\ -y & x & 0 \\ 0 & 0 & r \end{pmatrix}\begin{pmatrix} v_\perp \\ v_\parallel \\ v_z \end{pmatrix}, \tag{13}$$

where $r=\sqrt{x^2+y^2}$, and x and y are the coordinates of the boundary crossing particle. Equation (13) also makes the following shorthand notation possible:

$$\vec{v}^{ref} = \tilde{R}\vec{v}^{ran}. \tag{14}$$

This notation is used when discussing the numerical implementation of the collision rules. Since the reflected velocities are drawn out of distributions that correspond to the thermostat temperature, the next step is to select a strength of coupling to the heat bath. This coupling strength is determined by the frequency of diffuse collisions, i.e., the number of gas particles that are scattered diffusively per unit time. Such a coupling constant already exists for the Andersen thermostat and is denoted Γ [16]. As long as the gas particles are inside the cylinder, the potential energy of the gas particles is given by $U_p=\Sigma_j U_{p,j}=0$ and the following equation of motion is used:

$$\vec{r}(t+\delta t) = \vec{r}(t) + \vec{v}\Delta t, \tag{15}$$

where the position of the gas particle in three dimensions is given by $\vec{r}=(x,y,z)$. By switching off the Lennard-Jones interaction the only type of collisions that can occur are gas-wall collisions. This enables one to study the rarefied gas regime. Consider the nonperiodic xy-plane and form $r_j=\sqrt{x_j^2+y_j^2}$. As soon as gas particle j (with velocity $\vec{v}_j^{in}$) crosses the boundary, $r_j \geq \frac{d}{2} \rightarrow U_{p,j}=+\infty$, the following procedure is started:

(1) first the outward normal vector $\hat{n}_j$ is formed out of the particle coordinates (x_j,y_j);

(2) $\hat{n}_j$ is used to reflect the particle velocity specularly via Eq. (1); the particle position is updated in the xy-plane via $\vec{r}_j^{new}=\vec{r}_j(t_{end})+\vec{v}_j^{spec}\Delta t$, where $\vec{r}_j^{new}=(x_j^{new},y_j^{new})$. The position update resets the potential energy of particle j back to zero [see Fig. 2 and note that $r_n=\vec{r}\cdot\hat{n}$]. The specular collision (the velocity reflection plus the "momentum absorption" via the position update) also guarantees an orthogonal momentum transfer between the gas particle and the cylindrical wall of $\Delta(mv_{\perp,j})=2m(\vec{v}_j^{in}\cdot\hat{n}_j)$. The momentum transfer per collision is needed if one tries to evaluate the normal pressure of an ideal gas [14]. The z coordinate of particle j is not updated.

(3) A uniform random number, ζ, between 0 and 1 is drawn and compared with $\Gamma\Delta t$. If $\zeta<\Gamma\Delta t$, three new velocity components are drawn out of velocity distributions Eqs. (2) and (3) to form $\vec{v}^{ran}$. The matrix $\tilde{R}_j$ is formed out of the set (x_j^{new},y_j^{new}). The particle is assigned a new velocity with $\vec{v}_j^{new}=\vec{v}_j^{ref}=\tilde{R}_j\vec{v}^{ran}$. Without the position update in the previous step a particle could get stuck behind the wall (and stays there) if $\vec{v}_j^{ref}\cdot\hat{n}_j<\vec{v}_j^{in}\cdot\hat{n}_j$.

(4) The positions of the particles that have not crossed the wall are unaffected [12].

(5) $U_p=0$ and Eq. (15) is used again for all particles.

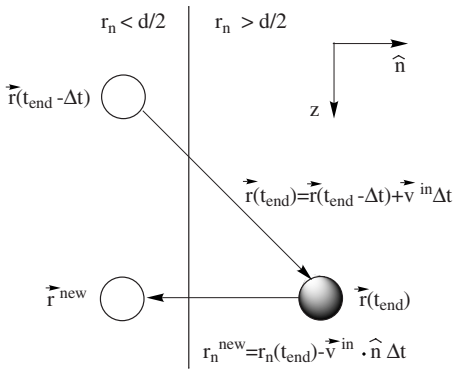

FIG. 2. Schematic representation of the boundary crossing. At time $t=t_{end}$ the particle has just crossed the thermal wall in one unit of time and the potential energy has become infinite. The velocity in the nonperiodic xy plane is updated via Eq. (1) and the normal component of the position at $\vec{r}(t_{end})$ is updated in order to bring the particle back to the other side of the wall and reset the potential energy back to zero (see step 2 of the procedure). At $\vec{r}^{new}$ the particle starts a new trajectory characterized by a new constant velocity in the nonperiodic xy plane.

III. SIMULATIONS

This research deals with a cylinder that was periodically copied in the z-direction containing 400 spherical gas particles. The reduced mass of the particles was fixed to $m^*=0.5$. The cylinder diameter is expressed in units σ, the atomic diameter, and has value $d^*=d/\sigma=12$. The length of the cylinder was chosen to be 125 units of σ. The unit of kinetic energy is k_BT, where k_B is the Boltzmann constant. The reduced wall temperature was fixed to $T_w^*=2.8$. If the gas particles interacted with each other through a Lennard-Jones potential this value would correspond with a temperature of $335K$ for argon. The reduced unit of time is $t^*=t/(\sigma\sqrt{m/k_BT})$ and the reduced velocity is given by $v^*=v\sqrt{m/k_BT}$. The time step used was $\Delta t^*=0.003$. Here $\Gamma\Delta t$ varied between 1 and 0.3. The physical quantities in this work are reported in reduced units denoted with an asterisk (*) [17]. They were calculated using a block average [18]. The length of each block varied between 4.2×10^4 and 2.7×10^5 time steps depending on the value of $\Gamma\Delta t$. Each block delivered two samples for the velocity auto correlation function (VACF). A typical run consisted of 600 blocks.

By counting the number of diffuse collisions in time per block and then computing the average over all blocks, a linear fit of the type $\nu^{diff*}t$ delivers the reduced diffuse gas-wall collision frequency, ν^{diff*}. This result was being compared with the expression that follows from kinetic theory considerations

$$\nu^{diff*} = \frac{N}{d^*}v^{thermal}\Gamma\Delta t, \tag{16}$$

where the thermal velocity is given by $v^{thermal}=\sqrt{\frac{8T_g^*}{\pi m^*}}$, $N=400$ and $T_g^*=T_w^*=2.8$. Figure 3 shows that the numerical simulations follow Eq. (16) very closely. The algorithm allows one to perform constant-temperature simulations. If $\Gamma\Delta t=1$ the number of diffuse collisions equals the total num-

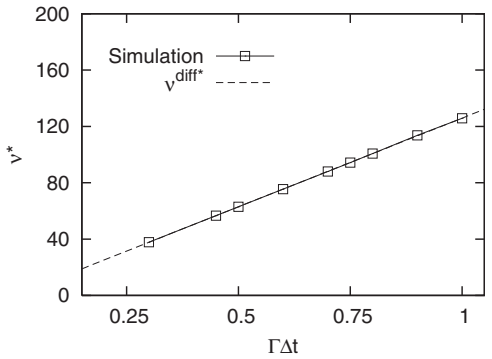

FIG. 3. Diffusive gas-wall collision frequency in reduced units as a function of $\Gamma\Delta t$.

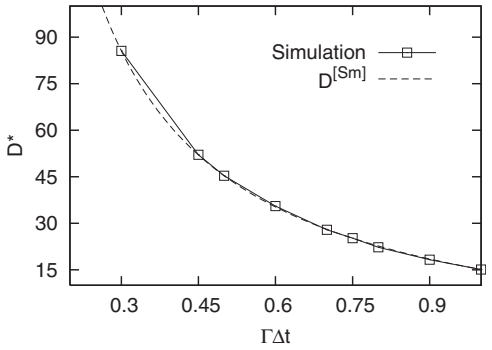

FIG. 4. Self-diffusion coefficient in reduced units as a function of $\Gamma\Delta t$.

ber of gas-wall collisions. Thus the quantity $\Gamma\Delta t$ is the fraction of total collisions which are diffusive. A final test for the boundary condition is the coefficient of self-diffusion of an ideal gas confined within a cylindrical thermal wall. The reduced self-diffusion coefficient is calculated with the Green-Kubo integral [19]

$$D_s^* = \lim_{\tau\to\infty} \int_{t=0}^{\tau} \langle v_z^*(t) v_z^*(0)\rangle dt, \tag{17}$$

where the value of τ is the cutoff time defined as the time it takes the VACF to decay to zero. If τ is chosen not large enough, a slightly smaller value of D_s^* will be measured. In practice, a short simulation determined the value of τ. Depending on the value of $\Gamma\Delta t$, τ varied between 2.8×10^4 and 1.8×10^5 time steps. To improve statistics even further, averages are taken over 12 independent simulations. The VACF is sampled every 25–150 time steps, depending on the size of τ. Gas wall collisions are fully responsible for the decorrelation of the VACF because there is no force term present in Eq. (15). In Fig. 4 D_s is plotted in reduced units as a function of $\Gamma\Delta t$. The simulation results have also been compared with Smoluchowski's expression for self-diffusivity in reduced units

$$D^{[Sm]} = \frac{d^*}{3} v^{thermal} \left(\frac{2-\Gamma\Delta t}{\Gamma\Delta t} \right), \tag{18}$$

where $T_g^*=2.8$. Error bars are the size of the symbols. As can be seen in Fig. 4, the agreement between the two reduced quantities is excellent. In the limit $\Gamma\Delta t\to1$, Knudsen's expression for the coefficient of self-diffusion is obtained. Thus one concludes that $f=\Gamma\Delta t$.

IV. DISCUSSION AND CONCLUSIONS

The stochastic boundary condition for the cylindrical thermal wall has been derived on the basis of a simple geometric argument. An important parameter was the coupling constant to a heat bath, Γ, which determines if a particle that has crossed the thermal wall is selected to undergo a diffusive collision. To test whether the boundary condition was correct the coefficient of self-diffusion of an ideal gas has been calculated using the time-correlation formalism. Numerical simulations then showed that Smoluchowski's result was recovered in reduced units. These simulations also revealed that the quantity $\Gamma\Delta t$ equals the tangential momentum accommodation coefficient f. Here f was an input parameter and does not need to be calculated. Interestingly, no intermolecular potential, like the Lennard-Jones interaction, was needed to reach the conclusion of the Smoluchowski model [Eq. (18)]. The method makes it is possible to simulate gas flows in nanotubes. The algorithm is a computationally cheap procedure for sampling the *NVT* ensemble, while obeying the physical theory constructed by Maxwell, Knudsen and Smoluchowski.

ACKNOWLEDGMENTS

The author is grateful to J. Valentijn for many fruitful discussions and L. L. van Benthem, D. Smid, and J. F. A. K. van Benthem for carefully reading this manuscript.

[1] S. Jakobtorweihen, M. G. Verbeek, C. P. Lowe, F. J. Keil, and B. Smit, Phys. Rev. Lett. **95**, 044501 (2005).
[2] S. Jakobtorweihen, C. P. Lowe, F. J. Keil, and B. Smit, J. Chem. Phys. **127**, 024904 (2007).
[3] A. I. Skoulidas, D. M. Ackerman, J. K. Johnson, and D. S. Sholl, Phys. Rev. Lett. **89**, 185901 (2002).
[4] J. H. Ferziger and H. G. Kaper, *Mathematical Theory of Transport Processes in Gases* (North-Holland Publishing, Amsterdam, 1972).
[5] M. Knudsen, Ann. Phys. **333**, 75 (1909).
[6] M. Knudsen, *The Kinetic Theory of Gases* (Methuen, London, 1934).
[7] M. Smoluchowski, Ann. Phys. **338**, 1559 (1910).
[8] R. A. Millikan, Phys. Rev. **21**, 217 (1923).
[9] G. Arya, H. C. Chang, and E. J. Maginn, Mol. Simul. **29**, 697 (2003).
[10] F. Celestini and F. Mortessagne, Phys. Rev. E **77**, 021202 (2008).
[11] J. L. Lebowitz and H. L. Frisch, Phys. Rev. **107**, 917 (1957).
[12] A. Tenenbaum, G. Ciccotti, and R. Gallico, Phys. Rev. A **25**,

2778 (1982).
[13] A. Tenenbaum, Phys. Rev. A **28**, 3132 (1983).
[14] R. B. Bird, W. E. Stewart, and E. N. Lightfoot, *Transport Phenomena* (John Wiley & Sons, Inc., New York, 2002), p. 39.
[15] R. Tehver, F. Toigo, J. Koplik, and J. R. Banavar, Phys. Rev. E **57**, R17 (1998).
[16] B. Smit and D. Frenkel, *Understanding Molecular Simulation: From Algorithms to Applications* (Academic Press, San Diego, CA, 2002), p. 142.
[17] J. M. Haille, *Molecular Dynamics Simulation: Elementary Methods* (John Wiley & Sons, Inc., New York, 1992), p. 113.
[18] B. Smit and D. Frenkel, *Understanding Molecular Simulation: From Algorithms to Applications* (Academic Press, San Diego, CA, 2002), Appendix D3.
[19] E. Helfand, Phys. Rev. **119**, 1 (1960).